REPORT DOCUMENTATION PAGE

AFRL-SR-AR-TR-04-

0103

1. AGENCY USE ONLY (Leave blank)

2. REPORT DATE 12/17/03

3. REPORT TYPE AND DATES COVERED Final: 12/1/00 – 11/30/03

4. TITLE AND SUBTITLE
Establishment of a Patrol Imager at AEOS for Space Weather and Mesospheric Studies

5. FUNDING NUMBERS
G# F49620-01-1-0064

6. AUTHOR(S)
Michael C. Kelley

7. PERFORMING ORGANIZATION NAME(S) AND ADDRESS(ES)
Cornell University
School of Electrical and Computer Engineering
318 Rhodes Hall
Ithaca, NY 14853

8. PERFORMING ORGANIZATION REPORT NUMBER

9. SPONSORING / MONITORING AGENCY NAME(S) AND ADDRESS(ES)
Office of Sponsored Programs
120 Day Hall
Cornell University
Ithaca, NY 14853

10. SPONSORING / MONITORING AGENCY REPORT NUMBER
38692

11. SUPPLEMENTARY NOTES

12a. DISTRIBUTION / AVAILABILITY STATEMENT
Approved for Public Release; distribution unlimited.

20040225 165

13. ABSTRACT (*Maximum 200 Words*)

Researchers at Cornell University have developed, implemented, and begun to reap scientific benefits of a dual camera/GPS system installed at the Advanced Electro-Optic System on Haleakala. This effort was a special AFOSR addition to the joint NSF/AFOSR Maui MLT initiative and constituted a major contribution by the AFOSR to the National Space Weather program. Images of unprecedented quality have been obtained detailing development and motion of severe convective ionospheric storms, ionospheric thunderstorms. These data have led to three *Geophysical Research Letters* publications, including one that was featured on the cover. One paper laid the groundwork for using future geostationary images of Space Weather phenomena by providing ground truth for orbital imaging of such storms. Two technology transfers were accomplished: airglow camera software was transferred to a national center, and a method for predicting severe Space Weather was transferred to the Air Force Research Laboratory. A statistical study in press has laid important groundwork for supporting the upcoming Air Force Communication/Navigation Outage Forecast System.

14. SUBJECT TERMS
Space weather, mesospheric/ionospheric structure, mesospheric bores

15. NUMBER OF PAGES 10

16. PRICE CODE

17. SECURITY CLASSIFICATION OF REPORT	18. SECURITY CLASSIFICATION OF THIS PAGE	19. SECURITY CLASSIFICATION OF ABSTRACT	20. LIMITATION OF ABSTRACT
Unclassified	Unclassified	Unclassified	UL

AFOSR Final Report

Establishment of a Patrol Imager at AEOS for Space Weather and Mesospheric Studies

F49620-01-1-0064

P.I.: Michael C. Kelley, Cornell University

Abstract

Researchers at Cornell University have developed, implemented, and begun to reap scientific benefits of a dual camera/GPS system installed at the Advanced Electro-Optic System on Haleakala. This effort was a special AFOSR addition to the joint NSF/AFOSR Maui MLT initiative and constituted a major contribution by the AFOSR to the National Space Weather program. Images of unprecedented quality have been obtained detailing development and motion of severe convective ionospheric storms, ionospheric thunderstorms. These data have led to three *Geophysical Research Letters* publications, including one that was featured on the cover. One paper laid the groundwork for using future geostationary images of Space Weather phenomena by providing ground truth for orbital imaging of such storms. Two technology transfers were accomplished: airglow camera software was transferred to a national center, and a method for predicting severe Space Weather was transferred to the Air Force Research Laboratory. A statistical study in press has laid important groundwork for supporting the upcoming Air Force Communication/Navigation Outage Forecast System.

I. Introduction

Installation of the Cornell Dual Camera system at the Advanced Electro-Optic System on Haleakala has been a great success. Unprecedented images of equatorial spread F plumes have been obtained during more than a year of nearly continuous operation. With it, we have laid the groundwork for interpreting data to be obtained from the Communication/Navigation Outage Forecast System scheduled for launch by the Air Force in 2004. This program is a high priority for the National Space Weather Program, a partnership of several government agencies that includes the Air Force Office of Scientific Research.

Scientific progress has been excellent. Three publications have been made in the prestigious *Geophysical Research Letters*. One of these papers was of sufficient interest to warrant a cover featuring the article.

More recently, the first year's accumulated airglow and GPS scintillation observations were compiled. This work lays the framework for using this system, along with other instrumentation in the mid-Pacific, to support the Air Force Communication/Navigation Outage Forecast System. This is a major Air Force initiative in the National Space Weather Program.

Two technology transitions have been made, one to Pennsylvania State University, which in turn has been passed on to a national center, and another to the Air Force Research Laboratory.

The instrumentation is described next, followed by abstracts of the relevant publications and selected data products.

II. Instrumentation

The original studies by *Rohrbaugh et al.* [1989] relied solely on the images from a narrow-field imager. The latter study by *Tinsley et al.* [1997] added information from two DMSP satellites and the San Marco satellite to put the images into a larger ionospheric context. However, no other ground-based instrumentation was available. For this current study, we have provided our own narrow-field imager and have added an all-sky imager, a dual-frequency GPS receiver to provide information on the total electron content of the ionosphere, and a single frequency GPS scintillation monitor. These four instruments combine to provide a more complete picture of the observed ESF than would be available from any one individual instrument and show the practical effects of ESF on satellite communication and navigation systems.

The images were taken by a dual CCD camera system deployed on top of the Haleakala Volcano on the island of Maui, HI. The first of the CCD cameras is the Cornell Narrow Field Imager (CNFI) consisting of a high-grade CCD (Photometrics 300 series) equipped with a telecentric lens system, a five-position filter wheel, and a 47° Mamiya primary lens. This camera is pointed southward along the magnetic meridian, similar to procedures used by previous researchers [*Rohrbaugh et al.*, 1989; *Tinsley et al.*, 1997]. The second CCD camera, the Cornell All-Sky Imager (CASI), is predominately the same as the narrow-field system except it uses a different CCD (Princeton Instruments) and has an all-sky (fisheye) primary lens. This camera is pointed to the zenith and can provide a horizon-to-horizon view of the sky. Generally, the all-sky camera at this location provides little information about the state of the equatorial ionosphere, but on nights of severe activity, such as that shown below, the midlatitude ionosphere can be severely disturbed by an equatorial phenomenon initiated over 2000 km away.

The two cameras image various emission lines naturally occurring in the nighttime ionosphere by selecting different narrowband filters in the filter wheel. Although there are many different emission lines that can be imaged, the two presented here occur at 557.7-nm and 777.4-nm. The 557.7-nm emission is the result of a two-step chemical reaction involving the neutral and charged species whereas the 777.4-nm emission is a simple one-step radiative recombination reaction involving only the ionospheric plasma [*Tinsley et al.*, 1973]. Consequently, the majority of the 557.7-nm emission occurs slightly below the peak of electron density in the ionosphere whereas the 777.4 emission occurs at the peak. In addition, the 777.4 nm is directly proportional to the square of the electron density. We also image the emission at 630.0 nm, but do not present any images here as they are significantly blurred due to the long lifetime of the reaction combined with the dynamical processes we are observing.

To augment the two cameras located on the Haleakala Volcano, we have also placed two Global Position System (GPS) receivers there. The first is a single-frequency (L1 at 1.5754 GHz) GPS receiver developed at Cornell University to record the signal power (at a 50 Hz sampling rate) of received GPS satellite signals [*Beach and Kintner*, 2001]. From these signal power measurements, the S_4 index can be calculated. The S_4 index is defined as the unity normalized standard deviation of the received signal power and is given by:

$$S_4 = \sqrt{\frac{\langle I^2 \rangle - \langle I \rangle^2}{\langle I \rangle^2}} \tag{1}$$

where I is the signal intensity and $<I>$ is the ensemble average of the signal power over a one-minute window [*Yeh and Liu*, 1982]. The second receiver is a NovAtel dual-frequency (L1, L2 at 1.2276 GHz) receiver, used to determine the total electron content (TEC) between receiver and satellite. Previous studies have shown a strong correlation between airglow and GPS-derived quantities [e.g., *Weber et al.*, 1996; *Kelley et al.*, 2000; *Makela et al.*, 2001].

As explained in more detail in *Tinsley* [1982], the island of Hawaii is situated ideally for observations of the height and longitudinal structure of the equatorial ionosphere. This is because of the high conductivity of the magnetic field lines, which allows for the efficient mapping of the effects of ESF above the equator to midlatitudes. If we assume that each of the emissions we are observing originate from a thin layer in the ionosphere (approximately one scale height below the F peak for 557.7 nm and 630.0 nm - typically 200 to 300 km during nighttime, and at the F peak for 777.4 nm) we can map the observed nightglow emissions to the magnetic equator. This geometry is shown in Figure 1a for the emission occurring at the F peak (777.4 nm) for a typical F-peak height of 350 km. Here we have assumed a dipole magnetic field, which is valid for the latitude range in question. The geometry will be similar for the two emissions with neutral dependencies (557.7 nm and 630.0 nm), but will map to slightly lower apex altitudes. Thus, the narrow-field camera provides a field-of-view that, when mapped to the magnetic equator, is equivalent to a height range of approximately 350 to 1000 km and a geomagnetic longitudinal range of 266 to 275 degrees east. The spatial resolution will be highest when the look direction is tangent to the magnetic field lines at the altitude of the emission layer. This was extensively studied in *Tinsley* [1982] and will not be repeated here.

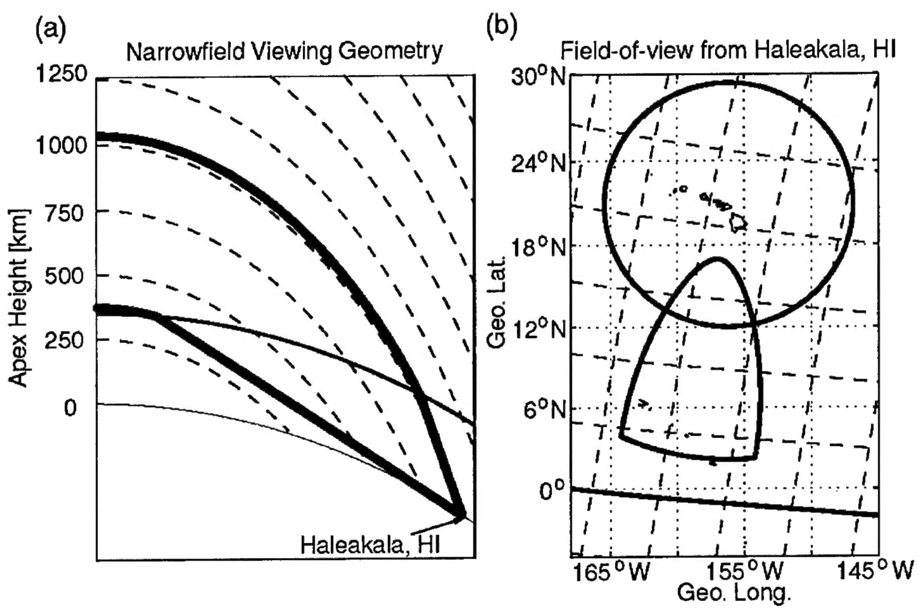

Figure 1. Geometry for viewing equatorial spread F from a midlatitude station. The field of view of a narrow-field camera (bold lines) map along magnetic field lines (dashed lines) to apex altitudes between approximately 350 and 1000 km. These altitudes will be slightly lower for emissions that occur at one scale height below the F peak, rather than at the F peak. (b) Fields of view for CASI (bold circle) and CNFI (bold arch) assuming an emission height of 350 km. Both geographic (dotted lines) and geomagnetic (dashed lines) coordinates are shown.

The all-sky camera gives us a horizon to horizon field of view that can be used to put any observations of ESF into a wider context. Although we do not expect to be able to observe much ESF using this camera (the spatial resolution at the horizon is not very good, see *Garcia* [1999]), we will be able to observe the development of the equatorial anomaly on nights of ESF compared to non-ESF nights. In addition, as shown below, especially spectacular ESF events are observed occasionally where the plumes extend to a higher equatorial height than can be observed by the narrow-field camera. On these nights, the all-sky camera acts as an extension to the narrow-field camera and provides an equatorial altitude range, albeit at lower spatial resolution, up to 2000 km. Figure 1b shows the fields of view of the two optical instruments projected to an ionospheric height of 250 km to give a better idea of the areas of the ionosphere that are being observed.

III. Scientific Results

Paper 1: Observations of equatorial spread-*F* from Haleakala, Hawaii, M.C. Kelley, J.J. Makela, B.M. Ledvina, and P.M. Kintner, *Geophys. Res. Lett.*, *29*(20), 2003, doi:10.1029/2002GL015509, 2002.

Abstract. Since the 1920s it has been known that the equatorial ionosphere can become highly disturbed in the post-sunset period. We have placed a new array of instruments on top of the Haleakala Volcano in Hawaii to study these disturbances from midlatitudes. Two airglow imagers provide two-dimensional snapshots of the development of these disturbances during the night, while two GPS receivers can quantify their severity. Here we report on the spectacular February 16-17, 2002 disturbance, which reached an altitude of 1500 km over the magnetic equator and mapped magnetically to latitudes well north of Hawaii. The signals from every Global Positioning System satellite in the field of view from Maui were severely disturbed whenever the corresponding look direction passed through one of the turbulent features. We also present an example from March 19, 2002 in which the spread-F activity is not as severe to demonstrate that the instrumentation still provides valuable information.

Figure 2 shows how the total system (all-sky airglow plus GPS receiver) can be used to study communications and navigational problems associated with convective ionospheric storms. Here we simultaneously see an image of the distance and, from the same location, the radiowave disturbance. Notice that whenever a GPS satellite line of sight passes through a dark region, scintillation of the signal is immediately initiated. Some is so severe that the satellite is not useful for navigational purposes. Since GPS is at gigahertz frequencies, any lower frequency system would be affected even more severely.

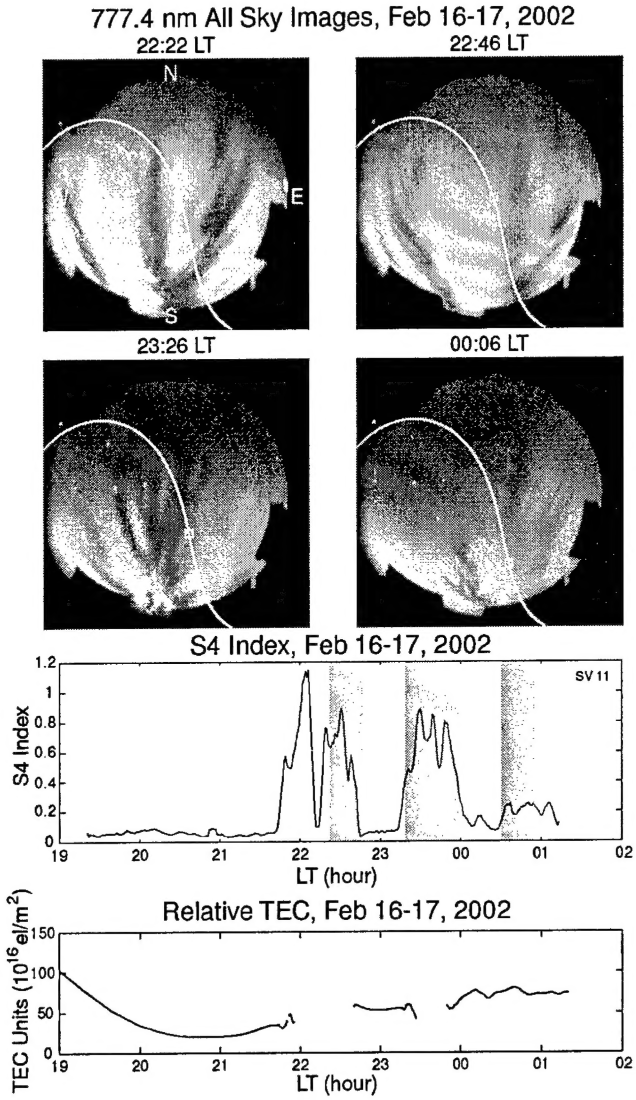

Figure 2. Four images taken with the Cornell All-Sky Imager of the 777.4 nm emission. GPS tracks for satellite 11 have been superimposed on the images. The square on each track denotes the location of the satellite when the image was taken. The middle panel shows the S_4 scintillation index recorded for satellite 11. The shaded times correspond to when the look direction to the satellite traversed through the depleted regions in the images. Note that no images were available before 2222 LT. The bottom panel shows the relative total electron content (TEC) as calculated by the NovAtel receiver. The data gaps correspond to times when the receiver lost lock on the L2 signal, rendering calculation of the TEC impossible.

Paper 2: Field-aligned 777.4-nm composite airglow images of equatorial plasma depletions, J.J. Makela and M.C. Kelley, *Geophys. Res. Lett.*, *30*(8), 1442, doi:10.1029/2003GL017106, 2003.

Abstract. We present a powerful tool to analyze two-dimensional field-aligned images of equatorial plasma depletions taken from mid-latitudes. By shifting each individual image by the sum of the longitudinal offsets obtained by performing a cross-correlation between successive images, a single composite image can be formed for the entire night. It is shown that these field-

aligned composite images give information on the observation times of the depletions associated with spread F as they pass by Hawaii. In addition, they can be used to estimate the formation time and location of the depletions to the west of the observing site. This technique also yields estimates of the eastward velocity and velocity shear of the depletions. We suggest that the information gained by using these images can be used to predict satellite scintillations at stations to the east of the observing station.

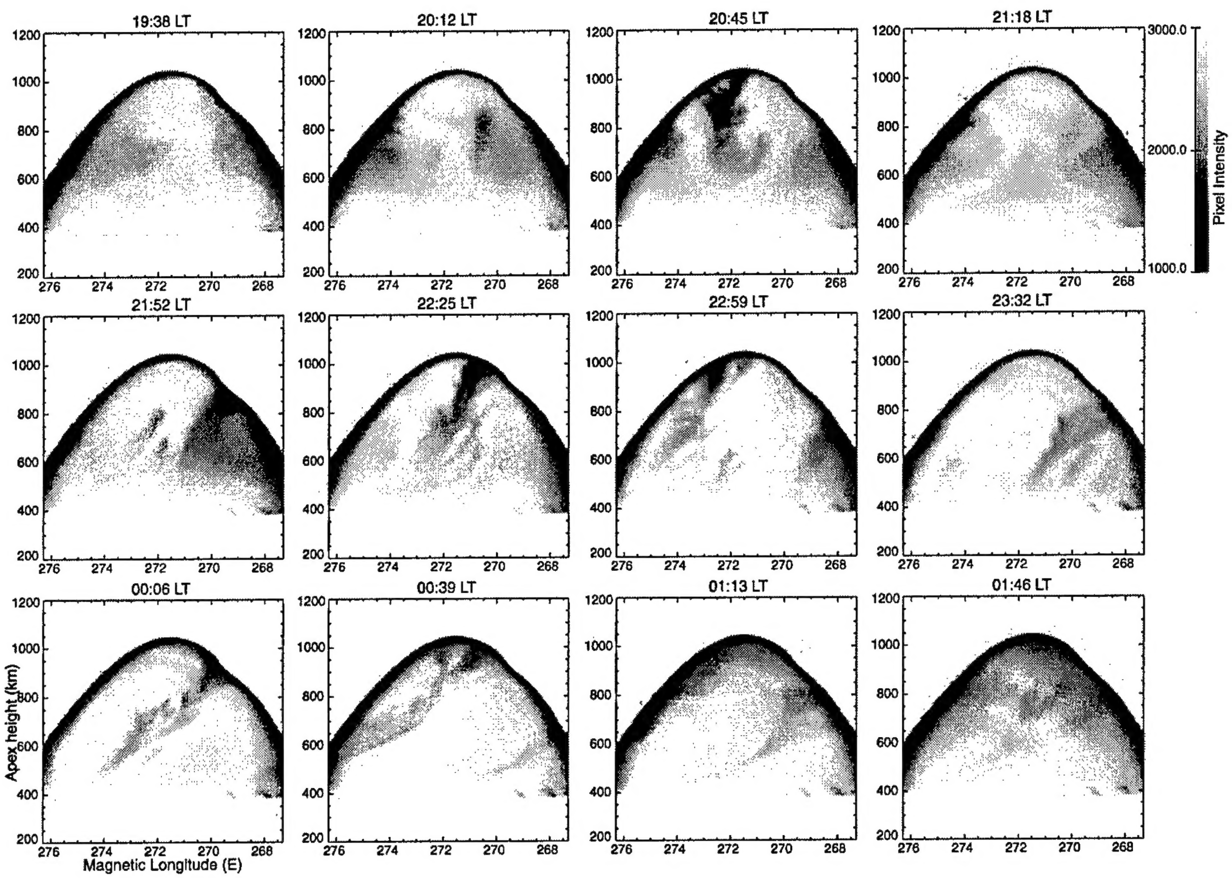

Figure 3. A sampling of 777.4-nm images taken on September 21–22, 2002. The image contrast for each image has been kept constant. The axes have been scaled such that the two axes are spatially consistent.

A sampling of one night's data is presented for reference in Figure 3. Every fifth image collected is shown here. The images have been projected along the magnetic field lines to the magnetic equator as described in *Kelley et al.* [2002]. The dark depletions seen in the images show the typical characteristics of equatorial spread-F (ESF) plumes or bubbles. They extend through the F layer into the topside, drift towards the east, and have a tendency to tilt westward with increasing height. Many common features can be seen in consecutive images, suggesting that a correlation could be performed to deduce the motion between the two frames. This is done for a slice through each image at a particular apex height (700 km in this paper). The choice of height is somewhat arbitrary, but a choice too high will miss some of the smaller bubbles, while one too low will run into problems due to the decreased brightness below the peak in intensity at

about 400–500 km. A correlation can be made when a similar feature exists (such as a bubble) in adjacent images and the longitudinal offset relating to the maximum correlation coefficient can be found. When a strong feature is not present, a linear fit is made between the two closest values of the longitudinal offset. By shifting each field-aligned image by the sum of the longitudinal offsets for the previous images and averaging, a composite image can be created. An example using the data presented in Figure 3 is shown in Figure 4. The x-axis label at the top of the composite image gives the local time at which each portion of the image was taken. The image is scaled such that both axes are spatially equivalent in the Hawaiian reference frame.

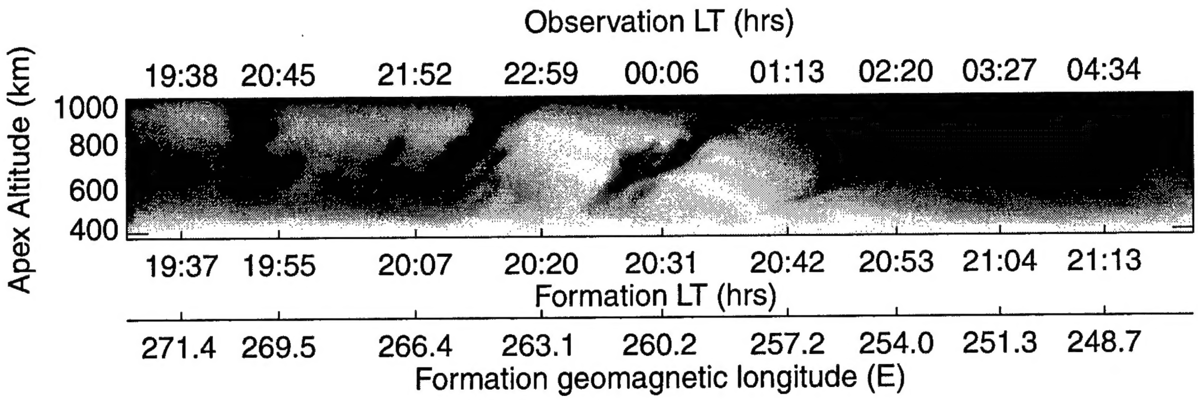

Figure 4. Composite image formed from images of the 777.4-nm emission taken on September 21–22, 2002. The top axis shows the time at which each portion of the image was taken. The bottom axis shows the estimate of the formation time and location of each portion of the image, assuming that each bubble formed 82 minutes after local sunset.

These field-aligned composite images give information on the observation time of the depletions at Hawaii, as well as estimates of the formation time and location of the depletions. In addition, information on the velocity shear can be obtained. The long-lasting nature of the depletion zones and the ability to estimate their velocity may provide a robust method for predicting satellite scintillations at stations to the east of the observing station. For example, detection of the second major bubble at 22:00 LT strongly indicates that scintillation would have occurred over Tahiti (geographic: -17.0°N, 210°E; geomagnetic: -15.9°N, 284.4°) at 02:00 LT. Recent observations of features identical to those in Figures 3 and 4 using the Global Ultraviolet Imager (GUVI) instrument on NASA's Thermosphere, Ionosphere, Mesosphere, Energetics, and Dynamics (TIMED) satellite [*Kelley et al.*, 2003] suggest that satellite-based imaging could make this predictive technique a global one.

Paper 3: The first coordinated ground- and space-based optical observations of equatorial plasma bubbles, M.C. Kelley, J.J. Makela, L.J. Paxton, F. Kamaladabi, J.M. Comberiate, and H. Kil, *Geophys. Res. Lett.*, *30*(14), 1766, 10.1029/2003GL017301, 2003.

Abstract. We report on ionospheric optical emissions detected by the GUVI instrument on the TIMED satellite. As the satellite crosses the equatorial zone the bright Appleton Anomaly region is imaged. Often these bright zones are interrupted by regions slanted from west to east as the equator is approached forming a backwards 'C'-shape in the image. To explain this feature we use simultaneous ground-based observations looking equatorward from Hawaii using the

777.4-nm emission. We also compare these optical observations to inverted electron density maps, as well as to those made by radar and to numerical simulations of the Rayleigh-Taylor instability. The characteristic shape is a result of a shear in the eastward plasma flow velocity, which peaks near the F peak at the equator and decreases both above and below that height. The ability to detect these unstable and usually turbulent ionospheric regions from orbit provides a powerful global remote sensing capability for an important space weather process.

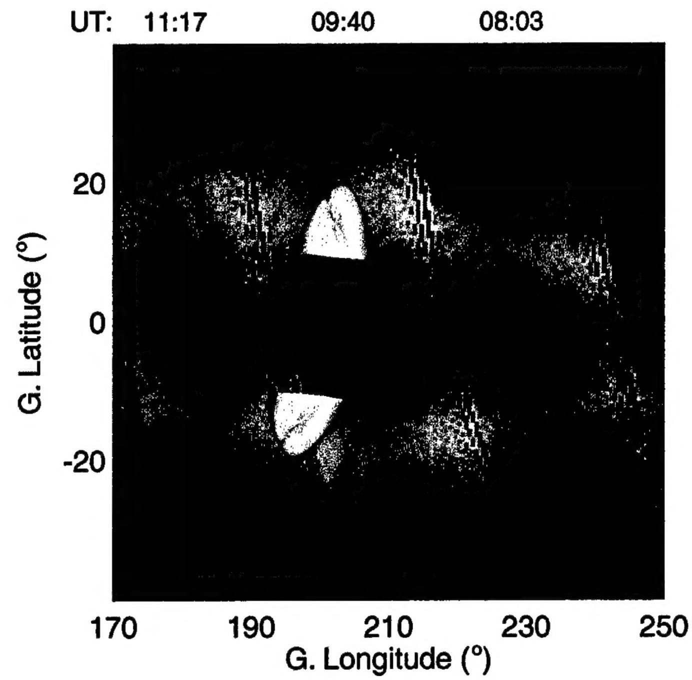

Figure 5. Comparison of the GUVI observations at 135.6-nm and ground-based observations at 777.4-nm.

The basic result is apparent in Figure 5, where we present data from September 22, 2002. The GUVI sweeps orthogonal to the ground track and images of the detected emissions can be created as shown in this figure. Quite often near the equator, the bright regions indicative of the anomaly regions are interrupted by dark bands which invariably slant westward with increasing value of the latitude in both hemispheres. On a few occasions these dark regions connect at the equator forming a backwards 'C'-shaped structure.

We have superposed the imager data on the GUVI data in the Pacific sector. The depletion over Hawaii is seen in both the GUVI data (red-scale image) and the narrow-field imager data (gray-scale image). The imager data were obtained approximately 20 minutes after the satellite data, so the fact that the darkened region is shifted slightly eastward is consistent with the eastward motion of the depletion.

The TIMED/GUVI data are totally consistent with ground-based radar and airglow data. They provide a new and powerful tool to study the global generation of ESF and its effects on Space Weather. Combined with ground-based observations, a full realization of the wedges can be gained. In addition, if coincident wedges were observed from space and the ground, the symmetry of the backwards 'C'-shape about the magnetic equator could be ascertained.

IV. Technology Transfer

A sequence of Cornell students has developed innovative software for remote sensing. This software has been freely offered to two universities and one system has been subsequently installed at a national center.

The predictive capability images have for severe Space Weather has been reported to the Air Force Research Laboratory. In addition, our results have been used to articulate the need for geostationary imaging of Space Weather processes analogous to such imaging of atmospheric processes.

References

Beach, T.L., and P.M. Kintner, Development and use of a GPS ionospheric scintillation monitor, *IEEE Transactions on Geoscience and Remote Sensing*, *39*(5), 918–928, 2001.

Garcia, F.J., *Atmospheric Studies Using All-Sky Imaging of Airglow Layers*, Ph.D. thesis, Cornell University, 1999.

Kelley, M.C., F. Garcia, J. Makela, T. Fan, E. Mak, C. Sia, and D. Alcocer, Highly structured tropical airglow and TEC signatitures during strong geomagnetic activity, *Geophys. Res. Lett.*, *27*(4), 465–468, 2000.

Kelley, M.C., J.J. Makela, B.M. Ledvina, and P.M. Kintner, Observations of equatorial spread-F from Haleakala, Hawaii, *Geophys. Res. Lett.*, *29*(20), 2003, doi:10.1029/2002GL015509, 2002.

Kelley, M.C., J.J. Makela, L.J. Paxton, F. Kamaladabi, J.M. Comberiate, and H. Kil, The first coordinated ground- and space-based optical observations of equatorial plasma bubbles, *Geophys. Res. Lett.*, *30*(14), 1766, 10.1029/2003GL017301, 2003.

Makela, J.J., and M.C. Kelley, Field-aligned 777.4-nm composite airglow images of equatorial plasma depletions, *Geophys. Res. Lett.*, *30*(8), 1442, doi:10.1029/2003GL017106, 2003.

Makela, J.J., M.C. Kelley, S.A. González, N. Aponte, and R. P. McCoy, Ionospheric topography maps using multiple-wavelength all-sky images, *J. Geophys. Res.*, *106*(A12), 29,175–29,184, 2001.

Rohrbaugh, R.P., W.B. Hanson, B.A. Tinsley, B.L. Cragin, and J.P. McClure, Images of transequatorial bubbles based on field-aligned airglow observations from Haleakala in 1984–1986, *J. Geophys. Res.*, *94*(A6), 6763–6770, 1989.

Tinsley, B.A., Field aligned airglow observations of transequatorial bubbles in the tropical F-region, *J. Atmos. Terr. Phys.*, *44*, 547–557, 1982.

Tinsley, B.A., A.B. Christensen, J. Bittencourt, H. Gouveia, P.D. Angreji, and H. Takahashi, Excitation of oxygen permitted line emissions in the tropical nightglow, *J. Geophys. Res.*, *78*(7), 1174–1186, 1973.

Tinsley, B.A., R.P. Rohrbaugh, and W.B. Hanson, Images of transequatorial F region bubbles in 630- and 777-nm emissions compared with satellite measurements, *J. Geophys. Res.*, *102*(A2), 2057–2077, 1997.

Weber, E.J., S. Basu, T.W. Bullet, C.E. Valladares, G. Bishop, K. Groves, H. Kuenzler, P. Ning, P.J. Sultan, R.E. Sheehan, and J. Araya, Equatorial plasma depletion precursor signatures and onset observed at 11 degrees south of the magnetic equator, *J. Geophys. Res.*, *101*(A12), 26,829–26,838, 1996.

Yeh, K.C., and C.H. Liu, Radio wave scintillations in the ionosphere, *Proc. IEEE*, *70*(4), 324–360, 1982.